UNIVERSITY of TASMANIA

University of Tasmania Open Access Repository

Cover sheet

Title
A Converging Slot-Hole Film-Cooling Geometry-Part 1: Low-Speed Flat-Plate Heat Transfer and Loss

Author
Jane Sargison, Guo, SM, Oldfield, MLG, Lock, GD, Rawlinson, AJ

Bibliographic citation
Sargison, Jane; Guo, SM; Oldfield, MLG; Lock, GD; Rawlinson, AJ (2002). A Converging Slot-Hole Film-Cooling Geometry-Part 1: Low-Speed Flat-Plate Heat Transfer and Loss. University Of Tasmania. Journal contribution. https://figshare.utas.edu.au/articles/journal_contribution/A_Converging_Slot-Hole_Film-Cooling_Geometry-Part_1_Low-Speed_Flat-Plate_Heat_Transfer_and_Loss/22842908

Is published in: 10.1115/1.1459735

Copyright information
This version of work is made accessible in the repository with the permission of the copyright holder/s under the following,

Licence.

If you believe that this work infringes copyright, please email details to: oa.repository@utas.edu.au

Downloaded from University of Tasmania Open Access Repository

Please do not remove this coversheet as it contains citation and copyright information.

University of Tasmania Open Access Repository

Library and Cultural Collections
University of Tasmania
Private Bag 3
Hobart, TAS 7005 Australia
E oa.repository@utas.edu.au CRICOS Provider Code 00586B | ABN 30 764 374 782 utas.edu.au

Proceedings of IGTI:
Turbo Expo '01
June 2001 New Orleans

2001-GT-0126

A CONVERGING SLOT-HOLE FILM-COOLING GEOMETRY PART 1: LOW-SPEED FLAT-PLATE HEAT TRANSFER AND LOSS

J.E. Sargison, S. M. Guo, M. L. G. Oldfield
Department of Engineering Science
University of Oxford
Oxford UK

G. D. Lock
Department of Mechanical Engineering
University of Bath
Bath UK

A. J. Rawlinson
Rolls Royce plc
Derby, UK

ABSTRACT

This paper presents experimental measurements of the performance of a new film cooling hole geometry - the *Converging Slot-Hole* or *Console*. This novel, patented geometry has been designed to improve the heat transfer and aerodynamic loss performance of turbine vane and rotor blade cooling systems. The physical principles embodied in the new hole design are described, and a typical example of the *console* geometry is presented.

The cooling performance of a single row of *consoles* was compared experimentally with that of typical 35° cylindrical and fan-shaped holes and a slot, on a large-scale, flat-plate model at engine representative Reynolds numbers in a low speed tunnel with ambient temperature main flow. The hole throat area per unit width is matched for all four hole geometries. By independently varying the temperature of the heated coolant and the heat flux from an electrically heated, thermally insulated, constant heat flux surface, both the heat transfer coefficient and the adiabatic cooling effectiveness were deduced from digital photographs of the colour play of narrow-band thermochromic liquid crystals on the model surface.

A comparative measurement of the aerodynamic losses associated with each of the four film-cooling geometries was made by traversing the boundary layer at the downstream end of the flat plate.

The promising heat transfer and aerodynamic performance of the *console* geometry have justified further experiments on an engine representative nozzle guide vane in a transonic annular cascade presented in Part 2 of this paper [1].

NOMENCLATURE

d Hole diameter
h Heat transfer coefficient
h_{mw} Heat transfer coefficient based on wall and mainstream temperatures
h_{nfc} Heat transfer coefficient without film cooling
H Boundary layer traverse distance
I_{actual} Actual Momentum flux ratio $= \dfrac{\rho_c v_c^2}{\rho_m v_m^2}$
I_{ideal} Ideal Momentum flux ratio $= \dfrac{P_{oc} - P_m}{P_{om} - P_m}$.
KE Kinetic energy flux $= \frac{1}{2}\dot{m}v^2 = \frac{1}{2}\rho v^3$
$\dot{m}$ Mass flux $= \rho v$
M Mass flux ratio, blowing ratio $M = \dfrac{\rho_c v_c}{\rho_m v_m}$
P Pressure
p Hole pitch
q Heat transfer rate from surface to flow
Re_d Reynolds number based on hole diameter and mainstream flow conditions, $\mathrm{Re}_d = \dfrac{\rho v d}{\mu}$
T Temperature
v Flow velocity
x, y, z Cartesian coordinates

Greek symbols

δ Displacement boundary layer thickness

Copyright © 2001 by ASME

η Film cooling effectiveness $\eta = \dfrac{T_{aw} - T_r}{T_{0c} - T_{0m}}$

ρ Density

θ Dimensionless temperature $\theta = \dfrac{(T_{0c} - T_{0m})}{(T_w - T_r)}$

Subscripts

aw Adiabatic wall
c Coolant
m Gas, mainstream
nfc No film cooling condition
o Total, stagnation conditions
r Recovery
w Wall

Abbreviations

Console Converging Slot-Hole
NGV Nozzle Guide Vane

Console Geometric Parameters

s exit throat slot height, controls coolant mass flow
w exit slot width, or *console* hole pitch
d inlet hole diameter
s_m solidity ratio, the proportion of metal left after hole has been drilled $s_m = \frac{1}{2}(1 - d/w)$
α hole inclination to surface
t wall thickness
l hole length $l = \dfrac{t}{\sin\alpha}$

INTRODUCTION

This paper presents low speed flat plate heat transfer and aerodynamic efficiency measurements of a new *console* cooling geometry. A companion Part 2 paper [1] extends these measurements to compressible flow on an engine representative nozzle guide vane (NGV).

Film cooling is widely applied in gas turbines to protect engine components from gas temperatures above the melting point of component materials. A considerable amount of research has been conducted in order to gain an understanding of the mechanisms involved in film cooling so that the design of film cooling systems can be optimised to produce the most effective film cooling with a minimum amount of coolant.

Minimising the aerodynamic loss associated with film cooling is also very important. Denton [2] suggests that, despite an estimated increase in turbine entry temperature of 100K per 1% coolant mass flow, a reduction of approximately 1% in turbine efficiency per 1% coolant flow can have a large effect on the overall cycle efficiency. This reduction is a viscous effect due to irreversible mixing of the coolant and mainstream flows.

Early work concentrated on the use of slots (e.g. Eckert and Drake [3]), which had the advantage of providing a uniform film that flowed along the downstream surface and did not introduce lateral thermal gradients, which can cause significant thermal stresses in engine components, reducing the life of the component. Farmer et al [4] have presented data for both straight and shaped inclined slots. Due to the practical structural difficulties associated with the use of slots on engine nozzle guide vanes and turbine blades, research and engine design practice have concentrated on using arrays of discrete holes to provide the most uniform film possible, without compromising the aerodynamic efficiency of the nozzle guide vane. Cylindrical holes, in single or double rows (Ligrani et al [5]), are often used with the holes directed downstream or with a compound angle in the plane perpendicular to the flow direction such as presented by Sen et al [6] and Schmidt et al [7]. Shaped film cooling holes are also used. Gritsch et al have presented heat transfer [8], and adiabatic effectiveness [9] measurements and Thole et al [10] have presented flow-field measurements for film cooling holes that expand laterally and/or forward near the hole exit. The purpose of the expansion is to increase the lateral spread of the coolant film downstream of the holes and to minimise the penetration of the coolant flow into the mainstream. While this shape improves the uniformity of the film over the surface compared with cylindrical holes, the hole expansion causes separation in the hole and inefficient diffusion, which reduce the aerodynamic efficiency of the NGV (Day et al, [11]).

CONSOLE

The new Converging Slot Hole, or *console*, film-cooling hole (patent applied for) described in this paper, has been designed to offer the improved cooling and aerodynamic performance of slot geometry, whilst retaining the mechanical strength of a row of discrete holes.

The cross-section of the *console* changes from a near circular shape at inlet to a slot at exit. In side view (Figure 1a) the walls of the *console* converge and in plan view (Figure 1b) the walls diverge, but the convergence is greater than the divergence so that the cross-sectional area decreases and the flow accelerates from inlet to outlet. The minimum hole area (throat) and hence maximum flow velocity are at the hole exit.

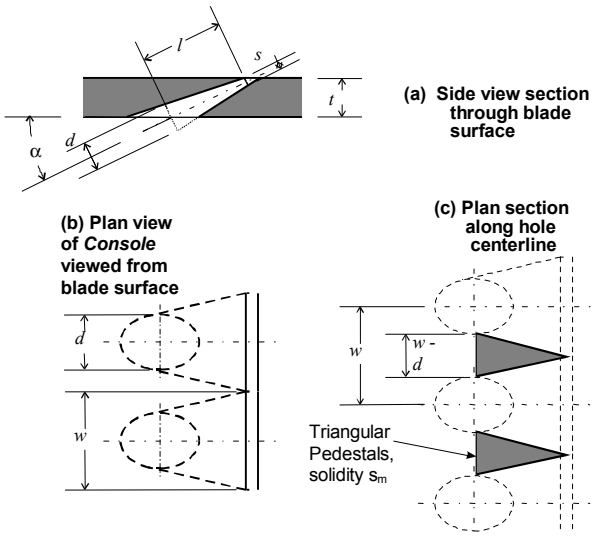

Figure 1: Basic *console* configuration

It has been widely established (eg [12]) that for accelerated flows, such the *console* internal flow, the boundary layer

Copyright © 2001 by ASME

generally remains laminar or turbulent boundary layers relaminarise whilst even a small amount of diffusion generally induces transition to turbulent flow. The losses due to turbulent flow are significantly higher than laminar flow. This is in contrast to conventional fan-shaped or expanded holes where the flow is diffused and slowed down in an attempt to spread the flow of the coolant onto the surface with low momentum. The separations in the fan-shaped hole [10], which reduce the aerodynamic efficiency of the fan-shaped holes, will be significantly reduced in the accelerating *console* flow. The low-turbulence exit flow from the *console* should lay a more stable layer of cooling air onto the external blade surface downstream of the exit and should reduce mixing of the coolant and the hot mainstream.

Individual holes in a row of *consoles* are positioned such that adjacent holes intersect just below the surface as shown in Figure 1, and a continuous slot is formed on the outside blade surface. The advantage of joining the hole exits is that the ejected coolant film is continuous in the span-wise direction (in contrast to cylindrical holes) and the film therefore benefits from the Coanda effect [12] and will not lift off from the blade surface at typical blowing rates. Evidence of the Coanda effect is described later in this paper.

The roughly triangular pedestals between holes (Figure 1) maintain the strength of the blade. To compare the structural integrity of the different cooling hole shapes, the minimum cross-sectional area of 25% for the particular *console* design used in the current work is reduced from 52% for the fan-shaped holes, and 67% for the cylindrical holes. The residual strength of the material with *consoles* should be sufficient, but further studies of the mechanical design of the *console* are required to verify this.

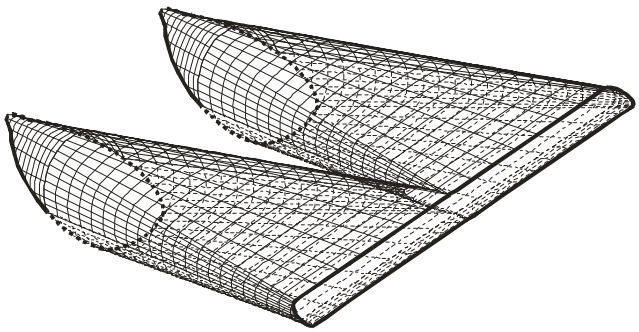

Figure 2: Uni Graphics surface definition of two *console* film cooling holes

The geometry of the basic *console* configuration has been designed to be generated from a family of straight lines as can be seen in Figure 2, and hence can be manufactured by available drilling (mechanical or laser) techniques. The hole entrance is nominally circular, but due to the way that the experimental *consoles* were generated, using straight lines, the hole entrance of the actual shape has a slight 'pen nib' effect as shown in Figure 2. As precision casting becomes more accurate, it will be possible to modify the basic *console* shape to further improve performance, such as detailed shaping of the hole entry and exit. The *console* patent application covers such improvements.

EXPERIMENTAL PROGRAM

As outlined above, heat transfer and aerodynamic loss measurements were carried out to quantify the performance of the *console*. The heat transfer experiments will be presented first, followed by the aerodynamic loss measurements.

HEAT TRANSFER MEASUREMENT

Experimental Technique

The experiments were performed in a 500x500 mm cross-section low speed, suck down wind tunnel [13] in the Osney Laboratory at the University of Oxford, shown in Figure 3. The mainstream (primary flow) air speed and temperature were measured upstream of coolant injection and these parameters were independent of the coolant flow. All measurements presented were conducted at engine representative Reynolds number (based on cylindrical hole diameter and mainstream flow) of 36000, ideal coolant to mainstream momentum flux ratio of 1.1 and density ratio of 1. The Reynolds number for every hole configuration was based on the cylindrical hole diameter for consistency in the presentation of results. The cylindrical hole diameter was 20 mm, the fan shaped hole inlet diameter was 24 mm, the slot height for the slot and *console* was 5 mm. By setting the holes pitch to be 60 mm for the cylindrical holes ($3d$), 84 mm for the fan-shaped holes ($3.5d_{\text{fan}}$), and 50 mm for the *consoles* ($2d_{\text{console}}$) equal throat area per unit width for each hole shape was achieved. For all data presentation, which required a hole diameter, the equivalent cylindrical hole diameter of 20 mm was used. For comparison with slot results, the Reynolds number based on the *console* and slot, slot height was 144000.

The ideal mainstream momentum flux ratio is equal to a pressure difference ratio $I_{ideal} = \dfrac{P_{0c} - P_m}{P_{0m} - P_m}$, and this was used as the basis for comparing coolant flows because it is this parameter that is set in the engine. The coolant total pressure P_{0c} is the total pressure measured in the coolant plenum, P_{om} is the total pressure of the mainstream flow measured upstream of coolant injection, and P_{m} is the static pressure of the mainstream measured at a wall static pressure tapping.

Although all holes were tested at the same pressure ratio, each hole geometry had a different discharge coefficient. This caused the mass flow rate, and hence velocity ratio and actual mass and momentum flux ratios to be different for each hole. The cylindrical hole mass flow rate was considered to be the standard mass flow rate and a hypothetical diameter, d_{hyp}, was defined for the other film cooling holes, which would produce the same mass flow rate as the cylindrical hole. For both

Copyright © 2001 by ASME

Figure 4: Typical film cooling hole configurations

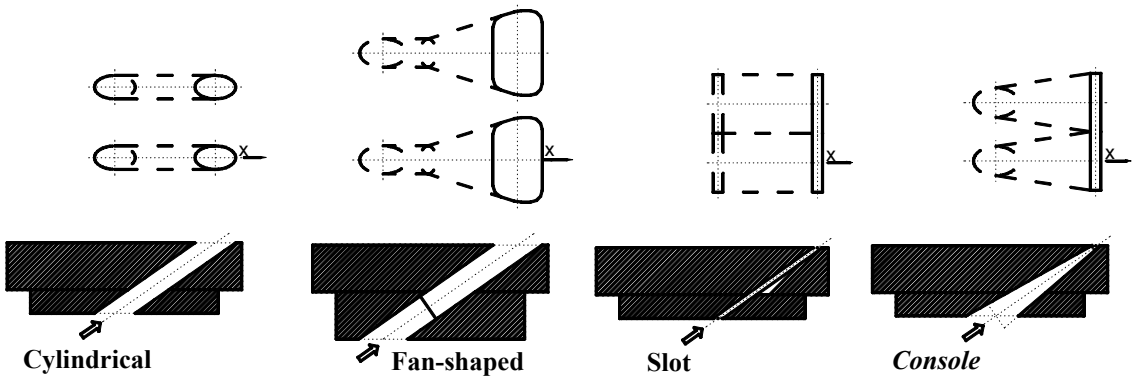

adiabatic effectiveness and heat transfer coefficient, the x parameter was corrected using:

$$x_{cor} = x\left(\frac{d_{hyp}}{d}\right), \qquad (1)$$

since the x scale for the effectiveness and heat transfer for a larger hole diameter would be equivalent when plotted against $\left(x/d\right)$.

The equation for heat transfer from a flat plate in uniform, turbulent flow [14] was manipulated to produce the following expression relating h and x, assuming that all other parameters are constant:

$$h \propto x^{-0.2} \qquad (2)$$

Since x is corrected as outlined above, the consequent correction in h can be written:

$$h_{corrected} = h\left(\frac{d_{hyp}}{d}\right)^{-0.2} \qquad (3)$$

The effectiveness scale does not require correction.

The mainstream flow velocity was 26 m/s and the freestream turbulence intensity was low, of the order of 1%.

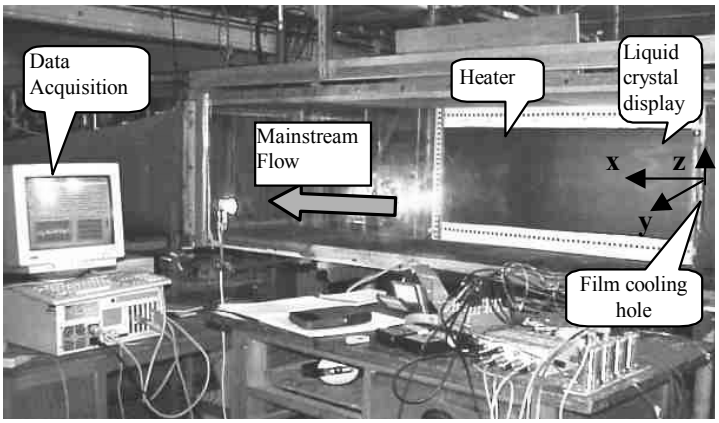

Figure 3: Osney laboratory low speed wind tunnel

The cooling air was supplied from the laboratory compressed air source and the mass flow rate of the air supplied to the plenum chamber was measured through a British Standard BS 1042 orifice plate (17.96 mm dia.). The air was heated using a variable power inline heater and fed into a plenum chamber to settle and mix the air before it exited through film cooling holes mounted in the side of the wind tunnel.

The film cooling holes were machined in cooling hole plates made from *Rohacell* type 51G - a closed pore, structural foam, manufactured by Rohm GMBH, with low thermal conductivity of 0.028 – 0.034 W/mK at 20°C, compared with air at 0.025 W/mK. A series of plates with the different film cooling hole geometries investigated were produced, and these could be easily changed in the experiment. There were five cylindrical holes and *consoles*, three fan-shaped holes and a single slot. The main geometrical features of the film cooling holes are shown in Figure 4.

A uniform heat flux flat plate, 1000 mm long, 600 mm wide and 30 mm thick (Figure 5) was produced from a large sheet of Rohacell backed with fibreboard for stiffness and covered with a 350 mm wide electrically heated thin film of aluminised Mylar, which was bonded to the surface with high strength double sided tape. The resistance of the thin film heating element quoted by the manufacturer was 2 Ω per square, but it varied slightly with temperature, so the voltage and current were measured in order to calculate the power supplied to the plate. The total resistance of the plate was 5.4 Ω at 18°C and the maximum heater power used was 200 W. The heat flux was uniform to within 3% over the surface of the plate. This plate was situated downstream of the film cooling holes.

The heating surface was painted black and narrow band thermochromic liquid crystals were used to measure constant temperature contours on the surface. Changing the coolant temperature or heat flux to the plate and allowing the system to settle to steady state conditions facilitated construction of a map of temperature contours.

A suite of Matlab routines were written to automatically calculate the heat transfer coefficient and adiabatic effectiveness at each point on the plate from the temperature contours. The temperature contours were extracted using the hue signal in the digital image, which was calibrated against temperature. The contour at a particular value of hue (where hue was most

Copyright © 2001 by ASME

sensitive to temperature) was captured using a Matlab routine, to obtain the temperature contour.

Film Cooling Analytical Technique

In the following discussion, total and recovery temperatures, appropriate to compressible flow, are used in order to present generally applicable equations and for consistency with the compressible experiments described in Part 2 of this paper [1]. Of course, in the incompressible experiments presented here, the total, recovery and static temperatures are equivalent.

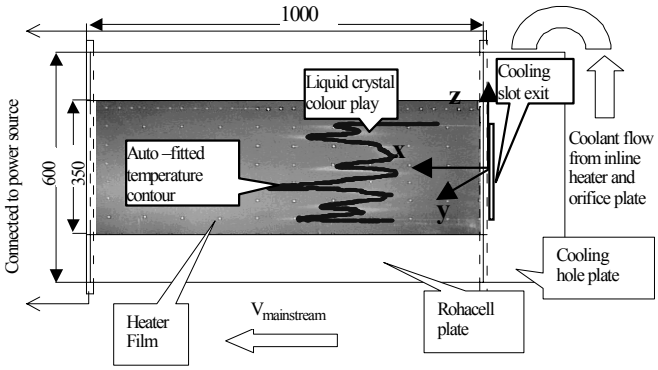

Figure 5: Tunnel wall showing layout of cooling holes and heated flat plate, overlaid with typical liquid crystal display with processed temperature contour.

The heat transfer coefficient, h, is defined following Jones [15,16] as the constant of proportionality between the local heat flux q and the difference between the wall temperature T_w and convection driving temperature of the gas T_{aw}, or *adiabatic wall temperature* at that point:

$$q = h(T_w - T_{aw}) \qquad (4)$$

For film cooling where there are two flows present, T_{aw} is intermediate between the coolant T_{oc} and mainstream T_{om} total temperatures and depends on these temperatures, the geometry and degree of mixing between the gases upstream of the point of interest on the surface. To eliminate the temperature dependence a dimensionless adiabatic film effectiveness is defined according to the definition of Jones [15,16]:

$$\eta = \frac{T_{aw} - T_r}{T_{0c} - T_{0m}} \qquad (5)$$

Here, T_r is the mainstream recovery temperature, which is defined using the recovery factor, $r = \mathrm{Pr}^{1/3}$, suggested by Kays and Crawford [14]:

$$T_r = T_{0\infty}\left(\frac{1 + r\frac{\gamma-1}{2}M^2}{1 + \frac{\gamma-1}{2}M^2}\right) \qquad (6)$$

The cooling effectiveness and heat transfer coefficients are primarily functions of cooling geometry, the state of the oncoming boundary layer, freestream turbulence intensity, surface curvature, and ratios of the coolant-to-mainstream density, mass and momentum fluxes, and specific heats [15]. Note the use of the recovery temperature T_r rather than T_{0m}.

To reduce the three controlling temperature variables in the experiment to a single parameter, a dimensionless temperature, θ, is defined:

$$\theta = \frac{T_{0c} - T_{0m}}{T_w - T_r} \qquad (7)$$

In experiments, an overall heat transfer coefficient h_{mw} based on the mainstream and wall temperatures is measured. If equations 2 and 3 are substituted into equation 1, then:

$$h_{mw} = \frac{q}{T_w - T_r} = h(1 - \eta\theta) \qquad (8)$$

This expression indicates that the variable h_{mw} is linear in θ. Furthermore, for a line relating h_{mw} to θ, h is the slope of the line and the intercept on the θ axis is $1/\eta$. A set of experimental points in (θ, h_{mw}) can be produced by varying the plate heat flux and coolant temperature.

The linearity of h_{mw} with θ was tested as part of the Matlab analysis sequence, by plotting h_{mw} against θ, for a number of positions on the plate. The typical results in Figure 6 show that good linearity was obtained.

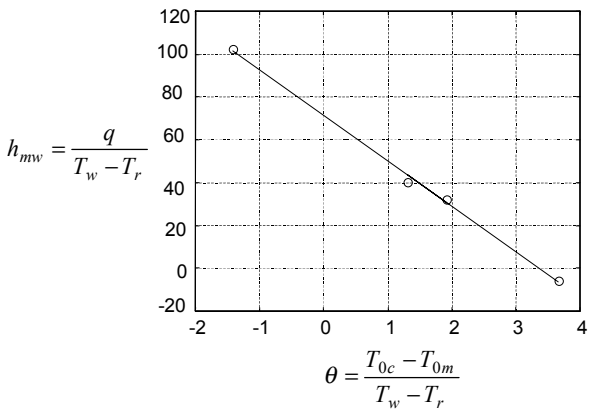

Figure 6: Typical set of data points and fitted straight line used in Matlab data manipulation

Downstream of a row of cooling holes, the effectiveness η varies periodically and previous workers (e.g. [5]) have simply arithmetically averaged η. Since h also varies, this is not technically correct and the correct method to calculate the lateral average is obtained by taking the average of both sides of Equation 5:

$$\overline{\left[\frac{q}{T_w - T_r}\right]} = \bar{h} - \overline{h\eta}\theta \qquad (9)$$

Thus the two properties of the film cooling heat transfer that are required for the average heat transfer prediction are $\bar{h}$ and $\overline{h\eta}$. The correct way to calculate the laterally averaged

Copyright © 2001 by ASME

effectiveness from the contour data, if it is to be used to determine the average heat transfer is:

$$\bar{\eta} = \frac{\overline{h\eta}}{\bar{h}} \qquad (10)$$

In practice, for moderate levels of heat transfer coefficient the difference between this definition and spatially averaged η is less than 5%

Results and Discussion

Experimental results were compared with previously published data to validate the current measurement technique. Good agreement between the current work and published results was obtained such as shown in Figures 7 and 8 for the cylindrical holes. The validation of the experimental technique by comparison with published results gives confidence in the subsequent *console* results. Note that the results are compared using the actual momentum flux ratio, I_{actual}, where the momentum flux of the coolant flow is defined:

$$\rho_c v_c^{\,2} = \frac{\dot{m}^2}{\rho} \qquad (11)$$

Throughout figures 7-12, the diameter, *d*, used for dimensionless distance is the equivalent cylindrical hole diameter of 20 mm. The dimension *z* for the lateral results in Figure 9 and 11 is made dimensionless by dividing by the hole pitch. The nominal slot pitch was made equal to the *console* pitch.

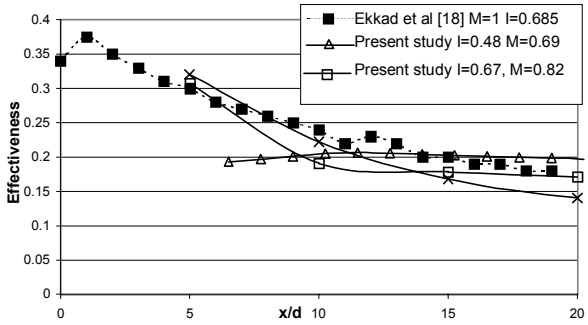

Figure 7: Cylindrical hole effectiveness compared with published data

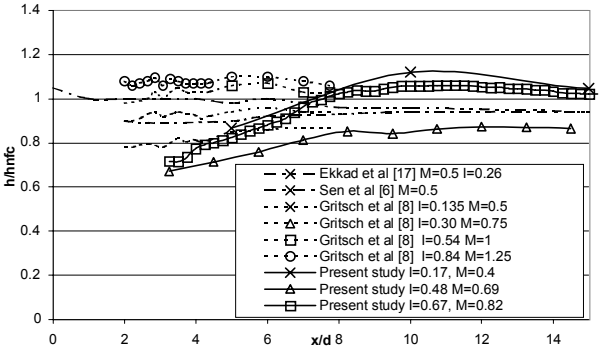

Figure 8: Cylindrical hole heat transfer coefficient compared with published data

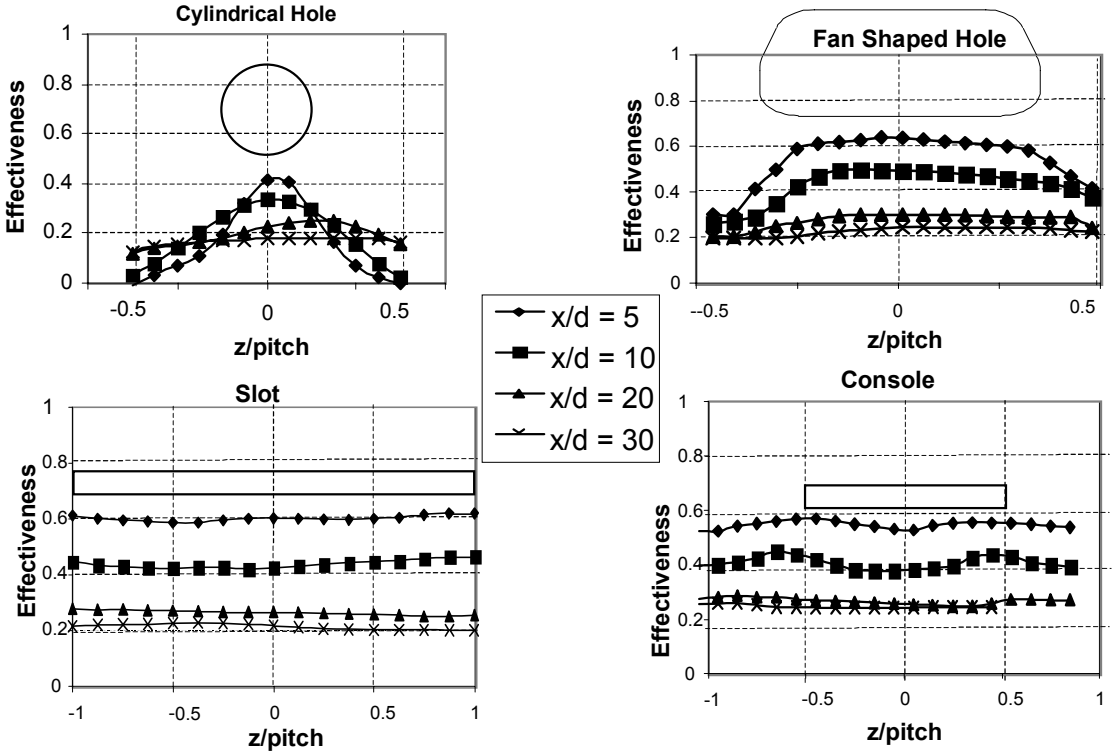

Figure 9a-d Lateral variation in adiabatic effectiveness, I_{IDEAL} = 1.1, Re_d = 36000

From a perturbation analysis of the effect of uncertainties in the measured parameters on the results of the curve fitting techniques, the uncertainty in *h* was estimated to be 8%, and the uncertainty in η was estimated to be 7%.

Copyright © 2001 by ASME

The lateral variation in adiabatic effectiveness for each film cooling geometry is presented in Figure 9a-d. As shown in Figure 5, the downstream distance x is measured from the downstream edge of the cooling hole or slot. The hole exit area is shown to scale on the graph. In this and all following charts, the x dimension is divided by the cylindrical hole diameter to provide consistency with the convention set by previous experimenters.

The cylindrical results show a pronounced peak in adiabatic effectiveness, η downstream of the hole centre. The peak is more spread for the fan shaped hole, as would be expected with the lateral expansion near the hole exit. The *console* result demonstrates a more uniform profile of η slightly enhanced at the intersection of two *consoles*. This enhancement is most likely due to interaction between vortices formed by the jets from adjacent *consoles*.

The slot effectiveness is similar to the fan and *console* peak effectiveness, which accounts for the similarity in the laterally averaged results for these film-cooling holes (Figure 10). The peak η values for the cylindrical holes are lower and reduce rapidly away from the holes, which accounts for the considerably lower laterally averaged effectiveness results.

The level of the lateral heat transfer coefficient shown in Figure 11a-d is similar for the slot and the *console* film cooling holes, and relatively uniform across the hole.

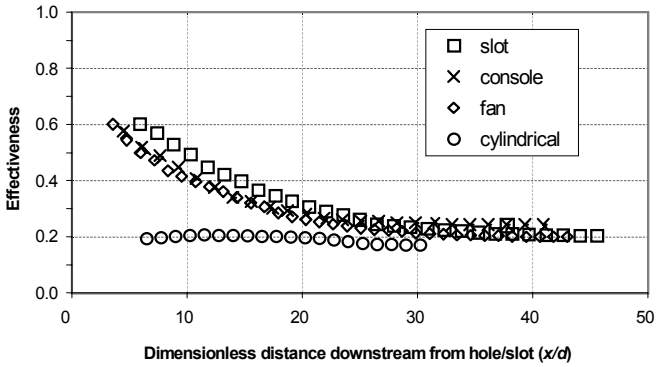

Figure 10: Laterally averaged adiabatic effectiveness, I_{IDEAL} = 1.1, Re_d = 36000

This demonstrates that the *console* flow is acting similarly to the slot. The heat transfer coefficient at exit from the fan shaped hole demonstrates only a small variation over the hole exit, and the level is markedly lower than for the slot and *console*. The cylindrical hole peak value is higher than the other cooling configurations, however h is lower between the holes, which contributes to the low laterally averaged heat transfer coefficient shown in Figure 12.

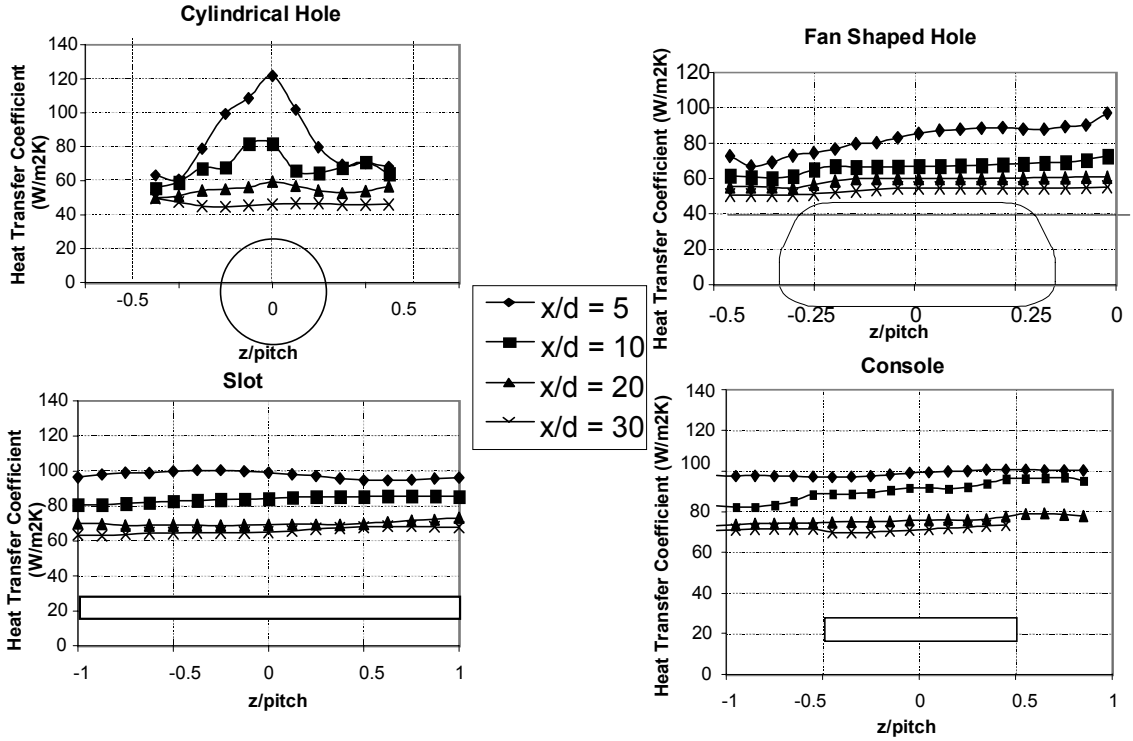

Figure 11a-d: Lateral variation in heat transfer coefficient, I_{IDEAL} = 1.1, Re_d = 36000

Copyright © 2001 by ASME

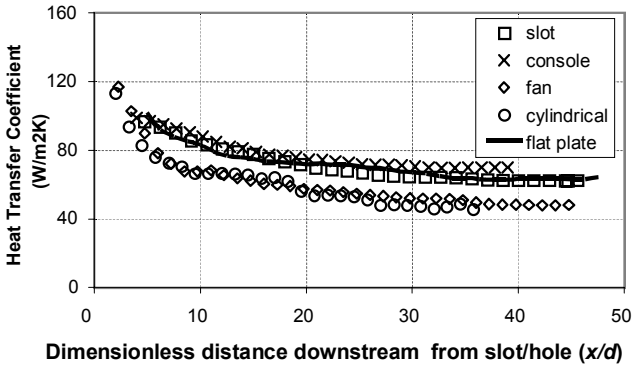

Figure 12: Laterally averaged heat transfer coefficient, I_{IDEAL} = 1.1, Re_d = 36000

The laterally averaged heat transfer results in Figure 12 demonstrate that the slot and *console* do not significantly change the boundary layer flow compared with no film cooling, and hence the heat transfer coefficient is similar. The fan-shaped and cylindrical film cooling holes appear to thicken the boundary layer and reduce the heat transfer coefficient compared with no film cooling.

The heat transfer performance of the *console* has been shown to be similar to the slot and fan film cooling performance. Aerodynamic loss measurements presented in the following sections are required in order to fully demonstrate the benefits of the *console*.

AERODYNAMIC LOSS

Experimental Technique

The measurement of aerodynamic loss was conducted using the tunnel equipment outlined above for the heat transfer measurement, except that there was no heat applied to either the heater film or the coolant. The boundary layer velocity and total pressure profiles were measured with a horizontally traversing pitot probe at the downstream edge of the plate, at positions downstream of a hole centre and halfway between two holes.

Analytical Technique

Aerodynamic loss is defined as 1-ε, (Day et al [11]) where the aerodynamic efficiency, ε, is defined:

$$\varepsilon = \frac{\{Actual\ Kinetic\ Energy\}_{mixingplane}}{\{Theoretical\ Kinetic\ Energy\}_{available}} \qquad (12)$$

The mixing plane is defined as the hypothetical plane at which the coolant and mainstream flows are fully mixed and the velocity, pressure and temperature are uniform. It is mathematically equivalent to the measurement plane and the velocity, static pressure and temperature at this plane are found by applying the laws of conservation of mass, momentum and energy between the measurement plane and the mixing plane.

The boundary layer traverse at the measurement plane is extended to the width of the wind tunnel, less the boundary layer thickness on the far side as shown in Figure 13. Although the results of this measurement are dependent on the dimensions of this wind tunnel, the purpose of the current experiments is to produce comparative data only. In the engine, the height of a downstream traverse required to measure aerodynamic efficiency is one blade pitch.

Applying conservation of mass from the measurement plane to the hypothetical mixed out plane in Figure 13, assuming constant density (low speed flow):

$$\int_0^H v dy = H v_2 \qquad (13)$$

Applying conservation of momentum:

$$P_1 + \rho \int_0^H v^2 dy = P_2 + \rho H {v_2}^2 \qquad (14)$$

From these two relationships, the actual kinetic energy flux of the flow at the mixed out plane can be calculated:

$$KE_{actual} = \tfrac{1}{2} \dot{m} {v_2}^2 = \tfrac{1}{2} \rho_2 {v_2}^3 \qquad (15)$$

For incompressible flow, the theoretical kinetic energy flux, based on the initial total pressure and the calculated static pressure at the mixing plane can be written:

$$KE_{theoretical} = \frac{\dot{m}_m}{\rho_m}(P_{om} - P_2) + \frac{\dot{m}_c}{\rho_c}(P_{oc} - P_2) \qquad (16)$$

Such that the loss is finally written;

$$Loss = 1 - \frac{\tfrac{1}{2}\rho v_2^3}{\frac{\dot{m}_m}{\rho_m}(P_{om} - P_2) + \frac{\dot{m}_c}{\rho_c}(P_{oc} - P_2)} \qquad (17)$$

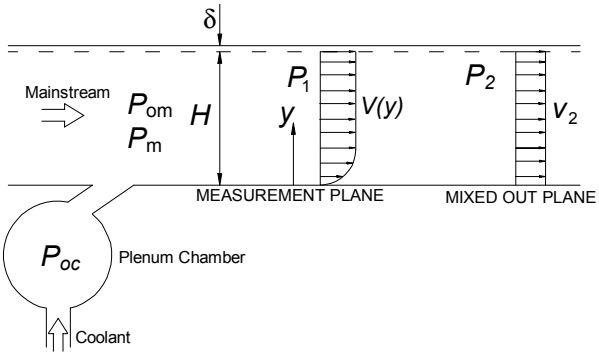

Figure 13: Measurement and calculation planes for aerodynamic loss

Results and Discussion

The usual coolant total pressure used for the calculation of aerodynamic loss is that measured in the cooling plenum. Day et al [11] point out that there are arguments for using either the coolant exit total pressure or the mainstream total pressure of which all three are presented here. The coolant total pressure at

Copyright © 2001 by ASME

the hole exit was calculated by Day et al [11] for the compressible case, which requires an iterative solution technique. For the incompressible case, an equation for P_{0c}, can be written:

$$P_{0c} = P_m + \tfrac{1}{2}\rho v^2_{exit} = P_m + \tfrac{1}{2}\frac{\dot{m}^2}{\rho} \qquad (18)$$

where P_m is the mainstream static pressure, the mass flux, $\dot{m} = \frac{measured\ mass\ flowrate}{A_{exit}}$, and A_{exit} is the exit area of the hole. For the fan shaped holes, the calculation of coolant exit total pressure is based on the nominal cross-sectional area of the expanded part of the hole at the hole exit plane, unlike Day et al [11] who use the hole throat area.

The aerodynamic loss measurements presented in Figure 14 clearly show the advantage of the *console* over the cylindrical and fan-shaped film cooling holes. The aerodynamic loss for the *console* is less than the slot and is even less than the no film cooling case. This is because the converging *console* hole flow has less internal loss than the straight slot. The cylindrical and fan-shaped film cooling holes have considerably higher aerodynamic loss.

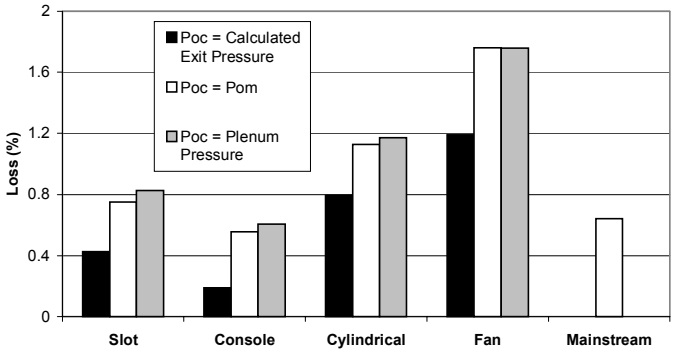

Figure 14: Comparison of aerodynamic loss of four cooling configurations, I_{IDEAL} = 1.1, Red = 36000

The difference between the calculated loss based on exit pressure and the total loss or loss based on plenum pressure is a measure of the loss through the film cooling hole. This is largest for the fan shaped hole, at 0.6% and smallest for the *console* at 0.35%. The large difference between these two results is due to the large loss associated with the inefficient diffusion process in the fan compared to the efficient, accelerating flow in the *console*. The two straight holes, the slot and cylindrical hole, exhibit a similar difference of 0.4%.

The uncertainty in these measurements was estimated to be 20% based on a 95% confidence level. The trends in loss outlined above remain valid with this level of uncertainty.

COANDA EFFECT INVESTIGATION

Evidence of the Coanda effect has been obtained in flow visualisation experiments using a nylon mesh coated with liquid crystals [19], which was positioned across the wind tunnel, one cylindrical hole diameter downstream of the film cooling holes. The experiment was conducted with jets in crossflow at the same I_{ideal} =1.1 as the other experiments presented in this paper, and jets without crossflow at the same pressure ratio across the hole. The contours extracted from images of the jet, clearly show that with no crossflow, the cylindrical hole jets lift off from the surface (shown as a dashed line in the figures) and with crossflow, the jets penetrate into the flow. For both situations, the *console* jets from the central three holes remain attached to the surface.

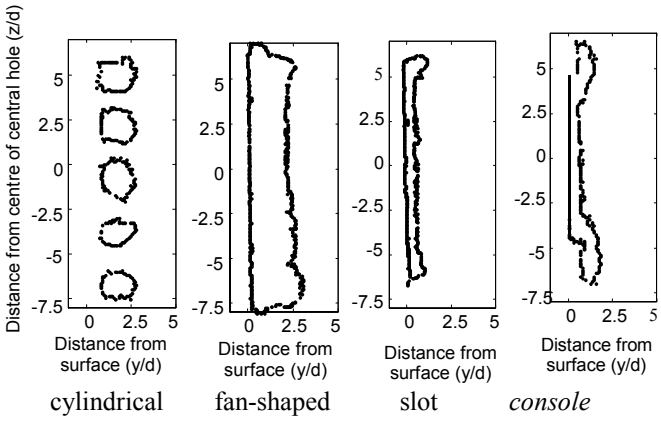

Figure 15: Film cooling hole jets contour without crossflow

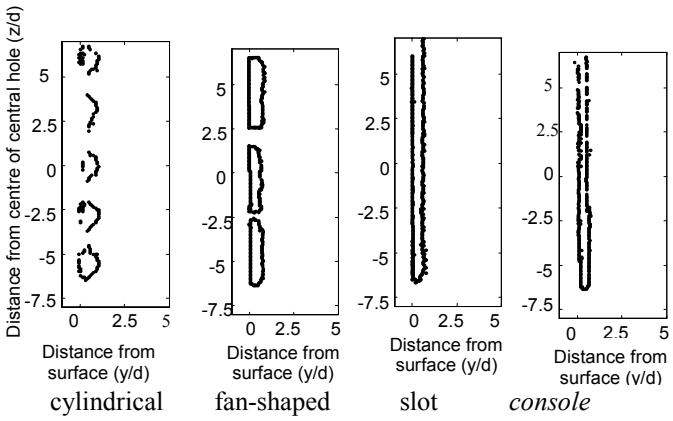

Figure 16: Film cooling hole jet contour with crossflow

CONCLUSIONS

The novel *console* film cooling hole shape has been presented and the thermal and aerodynamic performance has been compared with other conventional film cooling hole shapes. The coolant flow from a row of *consoles* shows good

Copyright © 2001 by ASME

lateral uniformity of adiabatic effectiveness, with regions of slightly enhanced cooling occurring between the *consoles* due to the interaction of vortices from adjacent holes.

The laterally averaged adiabatic effectiveness results demonstrate that the *console* approaches the slot effectiveness, as does the fan shaped hole effectiveness.

The *console* laterally averaged heat transfer coefficient was similar to the slot, and higher than the cylindrical and fan-shaped hole results. The slot and *console* do not significantly change the boundary layer flow compared with the case of no film cooling, and hence the heat transfer coefficient is similar. The fan-shaped and cylindrical film cooling holes appear to thicken the boundary layer and reduce the heat transfer coefficient compared with no film cooling. There is an aerodynamic penalty associated with this thickening.

The aerodynamic performance of the *console* was also investigated, and it was shown that the aerodynamic loss due to a *console* is significantly less than for fan shaped or cylindrical film cooling holes.

Hence, although these results indicate that the thermal performance of the *console* is similar to the fan-shaped film cooling holes currently in use, the *console* has a great advantage in terms of aerodynamic performance.

The promising results obtained from the flat plate experiments justify further experiments using the *console* geometry on a fully cooled nozzle guide vane under engine representative conditions which are presented in Part 2 of this paper [1].

ACKNOWLEDGMENTS

This work is supported by Rolls-Royce plc, DERA, DTI CARAD and MOD ARP26c.

REFERENCES

[1] Sargison, J.E., Guo, S.M., Oldfield, M.L.G., Lock, G.D., and Rawlinson, A.J., 2001, "A Converging Slot-Hole Film-Cooling Geometry. Part 2: Transonic Guide Vane Heat Transfer and Loss", ASME Paper 2001-GT-0127

[2] Denton, J.D., 1993, "Loss Mechanisms in Turbomachines", *Journal of Turbomachinery*, **115**, pp.621-656

[3] Eckert, E.R.G. and Drake, R.M., 1972, "Analysis of Heat and Mass Transfer", *McGraw Hill* pp 453-466

[4] Farmer, J.P., Seager, D.J., and Liburdy, J.A. 1997 "The Effect of Shaping Inclined Slots on Film Cooling Effectiveness and Heat Transfer Coefficient" ASME Paper 97-GT-399

[5] Ligrani, P., Ciriello, S., and Bishop, D.T. 1992 "Heat Transfer, Adiabatic Effectiveness and Injectant Distributions Downstream of a Single Row and Two Staggered Rows of Compound Angle Film-Cooling Holes", ASME Journal of Turbomachinery, **114**, pp. 687-700

[6] Sen, B., Schmidt, D.L. and Bogard D.G., 1996 "Film Cooling with Compound Angle Holes: Heat Transfer" ASME Journal of Turbomachinery, **118**, 800-806

[7] Schmidt, D.L., Sen, B. and Bogard, D.G., 1994, "Film Cooling with Compound Angle Holes: Adiabatic Effectiveness" ASME Paper 94-GT-312

[8] Gritsch, M., Schulz, A., and Wittig, S., 1998, "Heat Transfer Coefficient Measurements of Film-Cooling Holes with Expanded Exits" ASME Paper 98-GT-28

[9] Gritsch, M., Schulz, A., and Wittig, S., 1997, "Adiabatic Wall Effectiveness Measurements of Film-Cooling Holes with Expanded Exits" ASME Journal of Turbomachinery, **120**, pp. 560-567

[10] Thole, K., Gritsch, M., Schulz, A., and Wittig, S., 1996, "Flowfield Measurements for Film-Cooling Holes with Expanded Exits" ASME Journal of Turbomachinery, pp. 327-336

[11] Day, C.R.B., Oldfield, M.L.G. and Lock, G.D., 2000, "Aerodynamic Performance of an Annular Cascade of Film Cooled Nozzle Guide Vanes Under Engine Representative Conditions", *Experiments in Fluids,* **29**, pp. 117-129

[12] Schlichting, H., 1979, "Boundary-Layer Theory", McGraw-Hill Book Company, Seventh Edition, New York.

[13] Sargison, J.E., Guo, S.M., Oldfield, M.L.G., Lock, G.D., Rawlinson, A.J., 2000, "The Variation of Heat Transfer Coefficient, Adiabatic Effectiveness and Aerodynamic Loss with Film Cooling Hole Shape" *Proceedings of the Turbine-2000, International Symposium on Heat Transfer in Gas Turbine Systems,* Turkey

[14] Kays, W.M. and Crawford, M.E., 1993, *Convective Heat and Mass Transfer*, McGraw-Hill, New York.

[15] Jones, T.V., 1991, "Definition of Heat Transfer Coefficient in the Turbine Situation", IMechE 1991-3, C423/046, Turbomachinery: Latest Developments in a Changing Scene, pp. 201-206

[16] Jones, T.V., 1999, "Theory for the use of Foreign Gas in Simulating Film Cooling", International Journal of Heat and Fluid Flow, **20**, pp. 349-354

[17] Ekkad, S.V., Zapata, D. and Han, J.C., 1995 "Heat Transfer Coefficient over a Flat Surface with Air and CO2 Injection Through Compound Angle Holes Using a Transient Liquid Crystal Image Method" ASME Journal of Turbomachinery, **119**, pp. 580-586

[18] Ekkad, S.V., Zapata, D. and Han, J.C., 1995, "Film Effectiveness over a Flat Surface with Air and CO2 Injection Through Compound Angle Holes Using a Transient Liquid Crystal Image Method", ASME Journal of Turbomachinery, **119**, pp. 587-592

[19] Mee, D.J., Ireland, P.T. and Bather, S., 1999**,** "Measurement of the temperature field downstream of simulated leading-edge film-cooling holes", Experiments in Fluids, **27**, pp.273-283

 Copyright © 2001 by ASME